Journal of Fluorescence, Vol. 16, No. 3, May 2006 (© 2006)
DOI: 10.1007/s10895-005-0046-8

Relation Between Fluorescence Decays and Temporal Evolution of Excited States

János Erostyák,[1,2] Géza Makkai,[1] Andrea Buzády,[1] Péter Molnár,[1] and Sergei V. Kukhlevsky[1]

Received July 19, 2005; accepted December 5, 2005
Published online: February 14, 2006

A differential equation system describing the temporal evolution of excited substates and fluorescence emission were tested using a DOPRI algorithm. The numerical solutions show that there is significant difference in the measurable parameters according to the type of connectivity among the excited substates. In the globally connected case, the fluorescence emission exhibits a double exponential behavior, and the first moment of the emitted spectrum decays with stretched exponential characterized by $\beta < 1$. In the diffusive case the fluorescence emission cannot be always fitted with double exponential, and the first moment of the emitted spectrum may decay with stretched exponential characterized by $\beta > 1$. Details of modeling and the possibilities of drawing conclusions are also presented.

KEY WORDS: fluorescence decay; excited state relaxation; stretched exponential; numerical solution.

INTRODUCTION

Fluorescence is a powerful tool for collecting information from molecular level [1,2]. The decay of fluorescence emission is basically determined by the excited state processes. Several types of these processes are known, e.g., vibrational relaxation [3], dielectric relaxation, excited state reactions and many more. Their time-scale lasts from femtoseconds to nanoseconds and many times even towards the longer ranges. It is common in these processes, that their effects appear in the fluorescence decays and time-resolved spectra, generally resulting in nonexponential decays of fluorescence and a red- (or blue-) shift in the time-resolved spectra [4].

In this paper, a simple model is presented, in which simultaneous temporal evolution of excited states and fluorescence decays are followed. Different results are obtained depending on the initial conditions. This work was initiated by the observation of common fluorescence behaviors of different excited state relaxations.

In complex systems, such as proteins, polymers,biopolymers, colloid systems (emulsions and microemulsions), biological cells, porous materials, liquid crystals etc. the interconversion between a large number of states leads to complicated decays both in fluorescence emission and in the calculated first moment (also called center-of-gravity) of the spectrum [5,6]. There are several studies on the physical background of these decays. Protein conformational changes, and relaxations to thermal equilibrium in metallic nanoclusters also follow a stretched exponential law [7–10]. It was recently demonstrated that the inhomogeneity of coupling to the solvent of the bulk and surface atoms suffices to generate a spectrum of decay rates and a complex, nonexponential relaxation dynamics [11].

Among the huge number of articles modeling fast processes it is worth to note, that in numerical solutions the careful data handling is very important, sometimes an excellent-looking fit could catch the mind and may result in bad conclusions. Even a highly nonlinear experimental probe such as resonance energy transfer could exhibit a

[1] Department of Experimental Physics, Faculty of Sciences, University of Pécs, H-7624, Pécs, Ifjúság u. 6., Hungary.
[2] To whom correspondence should be addressed. E-mail: erostyak@fizika.ttk.pte.hu

decay that deviates from a simple exponential by less than 0.5% [8].

TERMS AND EXPRESSIONS

In our model, the excited state process will proceed as subsequent steps between excited substates separated by the same energy difference. The system will develop as a whole, jumping from substates to substates. At every time, the system can be described by the population distribution of excited substates. In the analysis of relaxation phenomena, it is a reasonable assumption that the rate of leaving a substate depends on the energy difference between the substates occurring in the single steps.

The results of calculations will depend on the type of connectivity between substates. Choosing different type of connectivity, the model allows to handle cases having different physical background [12,13]. In the "globally connected" case (GCC), every substate is accessible from every other, regardless of the energy difference between them. This global connection may happen via a higher transition state or directly, without any intermediate steps. The former can be observed in complex systems, e.g. proteins, where this higher energy transition state corresponds to a less compact form of the macromolecule and the helices are free to reposition. The latter happens e.g., in vibrational or dielectric relaxation of smaller fluorophores. In the "diffusive" case (DC), only transitions between initial and final substates that are neighbors in energy are allowed, i.e., $E_j = E_i \pm \delta E$. In this case, molecules move diffusively from the initial to the final distribution of population of excited substates.

$Y(n, t)$ denotes the population of nth substate of the excited state at time t. The first substate has the lowest energy, and the substates are separated by the same energy difference: $E_{i\pm1} = E_i \pm \delta E$. In the calculations we use $N = 30$ substates describing their temporal evolution in 501 time points. The fluorescence emission may occur from every substate. The spectral shape of emission from the nth substate at the emission frequency of ν is $EM(n, \nu)$. For practical considerations, the frequency steps between the points of the spectrum is choosen to be equal to the frequency difference of substates, i.e., $\delta\nu = \delta E/h$, where h is the Planck constant. In the spectral space 200 frequency points are used. The shape of the spectrum emitted from a higher or lower energy substate is the same, the difference is, that it is shifted towards the higher energies in case of a higher energy excited substate. Every single substate emits its own spectrum. The temporal evolution of nth substate's emission can be described as $Y(n, t)\ EM(n, \nu)$. The fluorescence decay at frequency ν and at time t will be a sum of emissions of different substates:

$$I(\nu, t) = \sum_{n=1}^{N} Y(n, t) EM(n, \nu). \tag{1}$$

The first moment of the excited substates

$$\overline{n}(t) = \frac{\sum_{n=1}^{N} Y(n, t) n}{\sum_{n=1}^{N} Y(n, t)} \tag{2}$$

and the first moment (center-of-gravity) of fluorescence emission

$$\overline{\nu}(t) = \frac{\sum_{\nu} I(\nu, t)\nu}{\sum_{\nu} I(\nu, t)} = \frac{\sum_{\nu}\left[\sum_{n=1}^{N} Y(n, t) EM(n, \nu)\right]\nu}{\sum_{\nu}\left[\sum_{n=1}^{N} Y(n, t) EM(n, \nu)\right]} \tag{3}$$

will be used in the analysis. The width of the observed spectrum $\Delta\nu$ is calculated as

$$[\Delta\nu(t)]^2 = \frac{\int I(\nu, t)(\nu - \overline{\nu})^2 \mathrm{d}\nu}{\int I(\nu, t)\mathrm{d}\nu} = \frac{\int I(\nu, t)\nu^2\,\mathrm{d}\nu}{\int I(\nu, t)\mathrm{d}\nu} - \left[\frac{\int I(\nu, t)\nu\,\mathrm{d}\nu}{\int I(\nu, t)\mathrm{d}\nu}\right]^2. \tag{4}$$

The master equation for the coupled differential equation system describing the evolution of excited substates is

$$\frac{\mathrm{d}Y(n, t)}{\mathrm{d}t} = \sum_{m=1}^{N} k_{mn} Y(m, t) - \sum_{m=1}^{N} k_{nm} Y(n, t) - \left(k_n^{\mathrm{r}} + k_n^{\mathrm{nr}}\right) Y(n, t), \tag{5}$$

where k_{mn} is the rate at which the molecules of mth substate converts to the nth substate, and expressed as follows:

$$k_{mn}(T) = k_0 g(E_n)\delta E \exp[-(E_n - E_m)/RT], \tag{6}$$

where $g(E_n)$ is the density of states at E_n, k_0 is a constant and $R = 8.31$ J/mol K. k_n^r and k_n^{nr} are the rates of radiative and nonradiative processes leading to the ground state. For simplicity, we assume that $g_{\mathrm{initial}}(E)$ and $g_{\mathrm{final}}(E)$ are identical Gaussian functions with the same standard deviation. It is a practical assumption, that the substates are separated by the same energy difference, this simplifies the differential equation system. In other words, we work with fixed separation between substates and uses $g(E)$, instead of using varying separation between substates. After excitation at $t = 0$, the equilibration of the system from the initial distribution of excited substates into the

final distribution is described by $Y(n, t)$. $k_{ii} = 0$ for $i = 1,\ldots, N$.

To solve (5), it is needed to give the initial population of excited substates $Y(n, 0)$, the k_{mn}, k_n^r, and k_n^{nr} rate constants, the $g(E_n)$ density of states and to set the possible ways of transitions between substates (GCC or DC).

The shape of emitted spectra could be chosen as a log-normal or a Gaussian function. The log-normal shape is characteristic for organic fluorophores such as quinine bisulphate, tryptophane, tyrosine and many others. Detailed description of these kind of spectra and the meaning of necessary parameters can be found in [14]. The Gaussian shape is also widespread among emitters.

DOPRI. The coupled differential equation system was numerically solved using the DOPRI algorithm, which belongs to the family of embedded Runge–Kutta methods. It was introduced by Dormand and Prince [15] and is very powerful and robust, ensuring short calculation times. The results were tested using different step lengths to be sure there are no artifacts within the results.

RESULTS AND DISCUSSION

The results of numerical evaluation will be shown parallel in the followings both in globally connected and diffusive cases, for the sake of comparability.

Temporal Evolution of Excited States

Figure 1 shows the temporal evolution of excited substates displaying their absolute values.

The substates converts towards the lower energies step by step. During the excited state relaxation every substate emits its own spectrum, which means, that at every time several substates are emitting. These elementary spectra have the same shape, but they are energetically shifted towards each other. The highest energy substate emits the bluest spectrum, the lower substates emit spectra shifted towards the lower energies, i.e., they are redshifted.

Fluorescence Decay Curves

When observing, we measure fluorescence intensity decay curves at fixed wavelegths, where the different parts of the elementary spectra originating from the different substates are added to each other. This is, what we can measure. The fluorescence intensity decays (Fig. 2) show the well-known shapes observable when the fluorescence spectrum is shifting in time.

In GCC, the most surprising fact is that these fluorescence decay curves can be fitted within not more than 0.1% error with double exponentials, in Fig. 2A–C the two lines are practically within the drawing linewidth. Moreover, the decay times τ_1 and τ_2 are constant along almost the whole spectrum, except at very low intensity ends of the spectrum. This is true for varying parameters of the elementary spectra in wide ranges. In case of elementary emission spectra of Gaussian shape even the low intensity parts of the total emission spectrum can be fitted with the same decay times (not shown in Fig. 2). On the blue side of the emission (Fig. 2A) both preexponentials are positive, around the middle of the spectrum (Fig. 2B) and on the red side (Fig. 2C) the shorter decay component has negative preexponential. The fitting parameters of the fluorescence decays of Fig. 2A–F can be seen in the inserts.

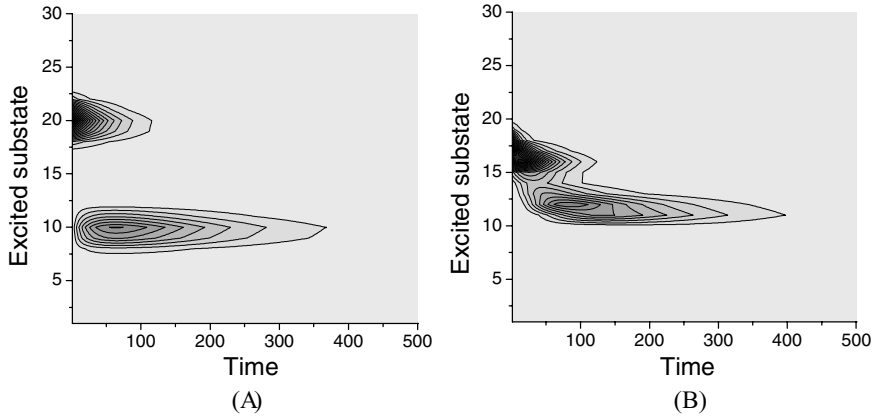

Fig. 1. Temporal evolution of excited states. (A) absolute intensities (GCC), (B) absolute intensities (DC).

In DC, double exponential can be found on the blue side and in the middle of the spectrum, but the shape of the decay is entirely different on the red side, where the fitting function varies according to the initial parameters, thus it cannot be given in a general formula for the decay function. A poor fit with double exponential can be seen in Fig. 2F.

General findings for both GCC and DC are that increase in the k_{mn} values results in faster transfer among substates, which yields a higher value for preexponential of the faster intensity-decay component. Similarly, decrease in the k_{mn} values results in slower transfer among substates, which yields a lower value for preexponential of the faster intensity-decay component. A less dramatic change in the preexponential of the slower intensity-decay component also appears.

First Moment of Excited Substates and Fluorescence Emission

Now, let us focus on temporal evolution of excited substates and total fluorescence described by the time dependence of their first moments $\overline{n}(t)$ (Fig. 3A and B) and $\overline{\nu}(t)$ (Fig. 4A and B), respectively.

Both of the first moment of excited substates and total fluorescence decay with the same function. This is obvious and is expected from the model we used [see Eqs. (2) and (3)]. When calculating the first moment of excited substates, these substates are weighted by their own populations. In case of the first moment of fluorescence emission, the picture is the same, because all of the excited substates emit the elementary spectra of the same shape.

The decay of first moments was found to be a stretched exponential:

$$\overline{n}(t) = \overline{n}(\infty) + c_n \exp[-(t/\tau)^{\beta}], \tag{7}$$

and

$$\overline{\nu}(t) = \overline{\nu}(\infty) + c_\nu \exp[-(t/\tau)^{\beta}], \tag{8}$$

where $\overline{n}(\infty)$ and $\overline{\nu}(\infty)$ are the first moments of excited states and the fluorescence emission, respectively, after infinitely long (practically: very long) time; c_n and c_ν are constants. This stretched relaxation is an average property of the ensemble.

In GCC, the molecules move towards the lower energies through jumps random in time and magnitude. The parameters of curves at (Figs. 3A and 4A) are $\tau = 51.33$ and $\beta = 0.946$. Of course, these numbers varies according to the initial parameter values, but it seems general, that in GCC $\beta < 1$. Usually, most of the systems characterized by stretched exponential behavior show $\beta < 1$.

In DC, the molecules relax in a relatively restricted way, thus the population moves as a group through the

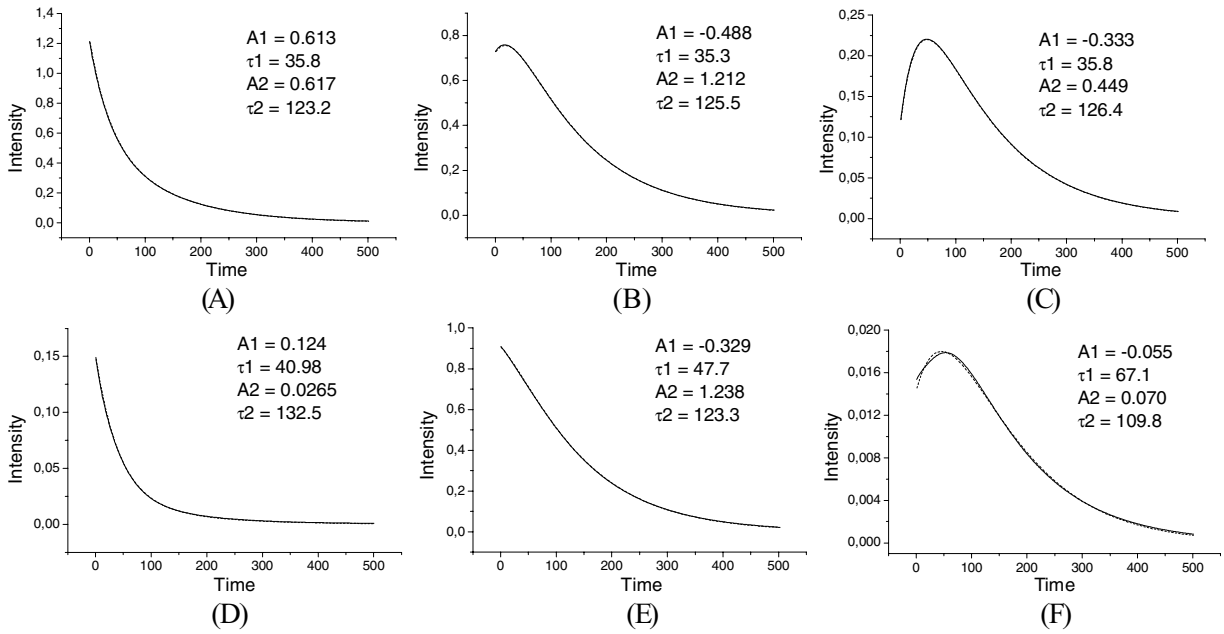

Fig. 2. Fluorescence decay curves. (A)–(C): GCC, (D)–(F): DC. The curves were produced using log-normal shape elementary emission spectra. Continuous line: decay originating from the model run; dashed line: double exponential fit for the decay. Insert: fitting parameters (preexponentials and decay times).

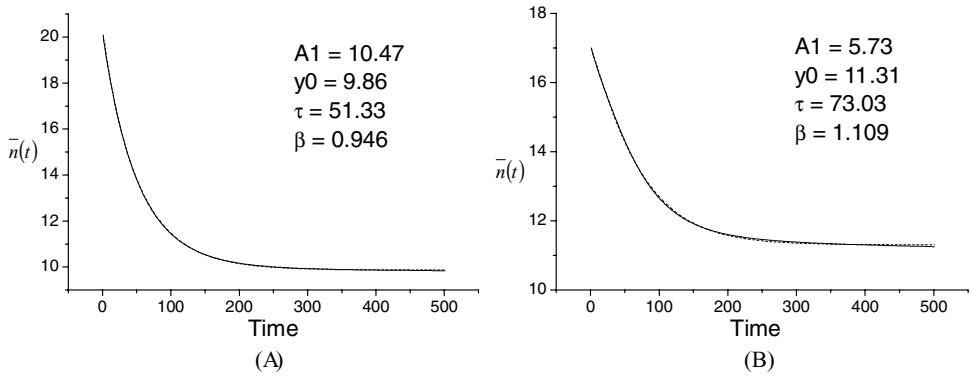

Fig. 3. Time dependence of the first moment of excited states. (A) GCC, (B) DC.

excited substates [see the contour plot in Fig. 1B]. The stretched exponential parameters of curves at Figs. 3B and 4B are $\tau = 73.03$ and $\beta = 1.109$. In DC, both $\beta < 1$ and $\beta > 1$ may occur depending on the circumstances. In the practice, $\beta > 1$ is relatively more rare; nevertheless, it also occurs [16].

Spectral Width

The last parameter we use now for describing the relaxation is the spectral width of fluorescence emission which has a maximum while the system moves from the initial towards the final distribution of excited substates.

Figure 5 shows the temporal evolution of the spectral width. Both in GCC and DC the spectral width increases first, then, after reaching a maximum value, decreases monotonically. In GCC, it can be fitted very well with double exponential at the wide ranges of initial parameters. In DC, the curve cannot be fitted so simply, it is far from a double exponential shape. In GCC the spectral width becomes wider at its maximum value than in DC. It is not surprising, because in GCC every substate is connected to every other substate, but in DC only the neighboring substates are connected; thus, the excited substate population moves as a narrower group through the possible substates.

CONCLUSION

Evolution of molecular excited substates were modeled with coupled differential equation system. The model allows to test different cases according to the type of connectivity between the substates.

In GCC, the fluorescence emission decays are predicted to be double exponentials having constant τ_1 and τ_2 decay times through the whole emission range. This reminds of a more simple system, namely the reversible excited two-state reactions, see, e.g., chapter 12 in [1], where also two constant decay times can be measured along the whole spectrum, but the preexponentials varies wavelength by wavelength. More or less, the system in GCC is very similar to that one. The difference is, that in our model there is an initial and a final distribution of excited substates all of them connected to each other, and

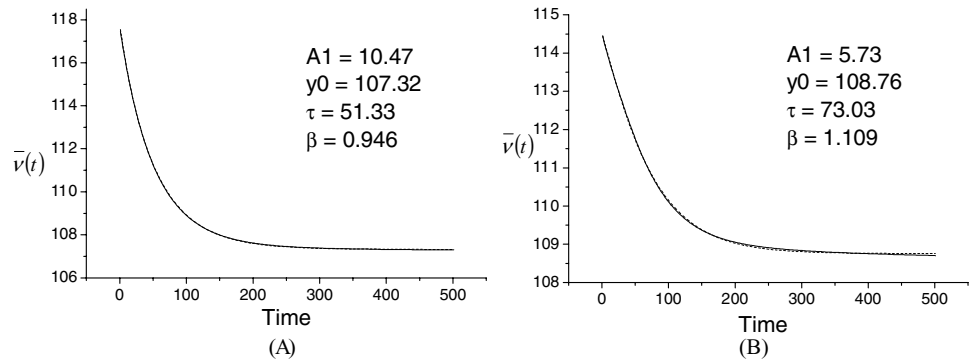

Fig. 4. Time dependence of the first moment of fluorescence emission intensity. (A) GCC, (B) DC.

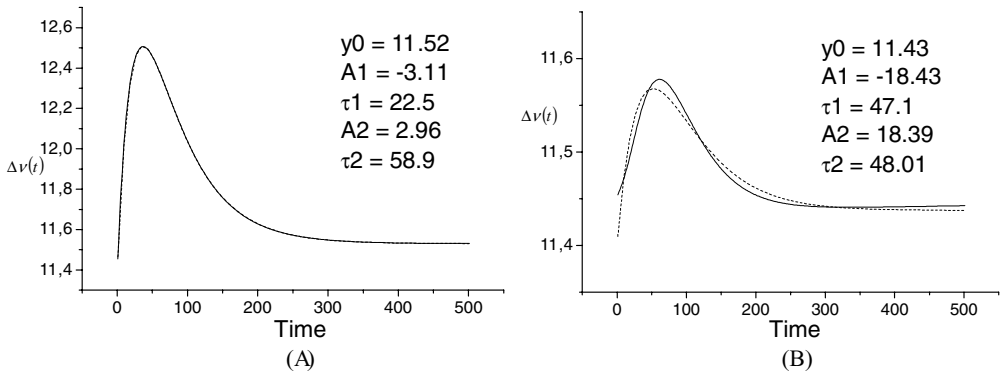

Fig. 5. Spectral width of fluorescence emission. (A) GCC, (B) DC.

not only two discrete excited states—belonging to excited monomer and dimer forms in that model.

Other example for application of our model is solvation relaxation, which can be described both by two-state model or by continuous model, too. The analysis of time-dependent spectral width (TDSW) helps us to distinquish between them. Examples for TDSW can be found in several articles, see [1,17,18]. A TDSW gives information about the underlying processes. If it practically does not change under the relaxation the continuous model fits well. If TDSW first increases, then decreases, the two-state—or it is better to say quasi two-state—model of relaxation is applicable. In our model, in GCC, the TDSW behaves as it is expected in two-state model of solvation relaxation.

The first moments of excited substates and of the fluorescence emission relax with an extended time course that can be fitted very well through a several order magnitude wide time range with a stretched exponential of $\beta < 1$. Nevertheless, let us not forget that the stretched exponential is only an empirical function, which is useful as an approximation of nonexponential data. At the time very near to zero, it gives an unrealisticly fast rate (it can be corrected using limiting rate modification of the formula). Similarly, after very long time, when only the slowest process dominates, several times the simple monoexponential could give a better fit.

In DC, the fluorescence decays on the blue side of the spectrum still are practically double exponentials, but on the red side they are not. The first moments show stretched exponential decay, but in many cases with $\beta > 1$. These features results from the fact, that in DC only the neighboring substates are connected, i.e., the jumps between the substates are very restricted.

It should be noted, that in our model system there is yet no barrier, e.g., dielectric relaxation (or solvation relaxation) and vibrational relaxation belong to this kind of systems. In a protein, the interconversion between various structures depends on the energy barrier. This situation can be modeled with our technique using the transition state mentioned in the section "Terms and Expressions." In this case, the sequence of the steps is as follows: starting substate—transition state—ending substate. Presently, we are working on calculations using this transition state in the model.

The simple model presented in this paper gives wide possibilities for fenomenological handling of the observed phenomena. It helps well to draw significant conclusions from the measured fluorescence decays even if not knowing all the details of the underlying physical and chemical processes. The further improvement and tests with results of biophysical measurements are on the way in our group.

ACKNOWLEDGMENTS

We thank Prof. Béla Somogyi, the Head of Institute of Biophysics at the University of Pécs for interesting and helpful discussions.

REFERENCES

1. J. R. Lakowitz (1983). *Principles of Fluorescent Spectroscopy*, Plenum Press, New York.
2. J. R. Lakowitz (1991). *Topics in Fluorescence Spectroscopy*, Plenum Press, New York.
3. M. Gruebele (1998). Intramolecular vibrational dephasing obeys a power law at intermediate times. *Proc. Natl. Acad. Sci. U.S.A.* **95**, 5965–5970.
4. D. Toptygin and L. Brand (2000). Spectrally and time-resolved fluorescence emission of indole during solvent relaxation: A quantitative model. *Chem. Phys. Lett.* **322**, 496–502.
5. K. Kuczera, J. C. Lambry, J. L. Martin, and M. Karplus (1993). Non-exponential relaxation after ligand dissociation from myoglobin. A

molecular dynamics simulation. *Proc. Natl. Acad. Sci. U.S.A.* **90**, 5805–5807.
6. Y. Feldman, A. Puzenko, and Y. Ryabov (2002). Non-Debye dielectric relaxation in complex materials. *Chem. Phys.* **284**, 139–168.
7. M. Lim, T. A. Jackson, and P. A. Anfinrud (1993). Nonexponential protein relaxation: Dynamics of conformational change in myoglobin. *Proc. Natl. Acad. Sci. U.S.A.* **90**, 5801–5804.
8. S. J. Hagen (2003). Exponential decay kinetics in "Downhill" protein folding. *PROTEINS: Struct. Funct. Genet.* **50**, 1–4.
9. J. R. Lakowicz (2000). On spectral relaxation in proteins. *Photochem. Photobiol.* **72**(4), 421–437.
10. J. Gapinski, M. Paluch, and A. Patkowski (2002). Correlation between nonexponential relaxation and non-Arrhenius behavior under conditions of high compression. *Phys. Rev. E* **66**(1), 011501.
11. F. Piazza, P. De Los Rios, and Y.-H. Sanejouand (2005). Slow energy relaxation of macromolecules and nanoclusters in solution. *PRL* **94**, 145502.
12. S. J. Hagen and W. A. Eaton (1996). Nonexponential structural relaxations in proteins. *J. Chem. Phys.* **104**(9), 3395–3398.
13. J. Sabelko, J. Ervin, and M. Gruebele (1999). Observation of strange kinetics in protein folding. *Proc. Natl. Acad. Sci. U.S.A.* **96**, 6031–6036.
14. E. A. Burstein and V. I. Emelyanenko (1996). Log-normal description of fluorescence spectra of organic fluorophores. *Photochem. Photobiol.* **64**(2), 316–320.
15. J. R. Dormand and P. J. Prince (1980). A family of embedded Runge-Kutta formulae. *J. Comp. Appl. Math.* **6**, 19–26.
16. H. K. Nakamura, M. Sasai, and M. Takano (2004). Squeezed exponential kinetics to describe a nonglassy downhill folding as observed in a lattice protein model. *PROTEINS: Struct. Funct. Bioinform.* **55**, 99–106.
17. R. P. De Toma and L. Brand (1977). Excited state solvation dynamics of 2-anilinonaphthalene. *Chem. Phys. Lett.* **47**, 231–236.
18. J. R. Lakowitz, H. Cherek, G. Laczko, and E. Gratton (1984). Time-resolved fluorescence emission spectra of labeled hospholipid vesicles, as observed using multi-frequency phase-modulatoin fluorometry. *Biochim. Biophys. Acta* **777**, 183–193.